Open access • Journal Article • DOI:10.1051/JPHYS:01982004303053900

On experimental attenuation factors of the amplitude of the EXAFS oscillations in absorption, reflectivity and luminescence measurements — Source link

J. Goulon, C. Goulon-Ginet, R. Cortes, Jean-Marie Dubois

Institutions: Pierre-and-Marie-Curie University

Published on: 01 Mar 1982 - Journal De Physique (Société Française de Physique)

Topics: Surface-extended X-ray absorption fine structure, Attenuation, Extended X-ray absorption fine structure and Harmonics

On experimental attenuation factors of the amplitude of the EXAFS oscillations in absorption, reflectivity and luminescence measurements

J. Goulon, C. Goulon-Ginet, Robert Cortès, J.M. Dubois

Classification
Physics Abstracts
61.10F — 61.16 — 61.60 — 61.40

On experimental attenuation factors of the amplitude of the EXAFS oscillations in absorption, reflectivity and luminescence measurements

J. Goulon (*), C. Goulon-Ginet (*), R. Cortes (**) and J. M. Dubois (***)

(*) Laboratoire de Chimie Théorique. ERA 22 au C.N.R.S. « Interactions Moléculaires », Université de Nancy I, Case Officielle 140, 54037 Nancy Cedex, France
et L.U.R.E. (†). Laboratoire Propre du C.N.R.S. associé à l'Université de Paris-Sud, Bâtiment 209C, 91405 Orsay, France

(**) Groupe de Recherche n° 4 (C.N.R.S.) « Physique des Liquides et Electrochimie » associé à l'Université Pierre et Marie-Curie, Paris VI, 4, place Jussieu, 75230 Paris Cedex 05, France

(***) Laboratoire de Métallurgie. LA 159 au C.N.R.S, E.N.S.M.I.N., Institut National Polytechnique de Lorraine, Parc de Saurupt, 54000 Nancy, France

(*Reçu le 12 août 1981, accepté le 10 novembre 1981*)

Résumé. — Cette publication examine un certain nombre d'artéfacts expérimentaux qui limitent généralement l'analyse des spectres EXAFS. Dans le cas des mesures conventionnelles par absorption, les principales sources d'erreurs sont d'une part, la transmission d'harmoniques par le monochromateur, et d'autre part, l'existence d'inévitables fuites de rayonnement autour ou au travers de l'échantillon. Il en résulte non seulement une altération de l'amplitude du signal mais encore une distorsion harmonique des oscillations d'EXAFS et une perturbation systématique des termes de Debye-Waller déterminés. Une correction efficace des effets dus plus précisément aux fuites de rayons X est proposée et il est suggéré de contrôler la présence ou l'élimination des harmoniques en suivant la reproductibilité des hauteurs des seuils lorsque l'on insère, derrière l'échantillon, des feuilles métalliques étalons de différentes natures. L'analyse fondamentale développée par les mesures par absorption a été étendue aux cas de la technique REFLEXAFS et d'autres techniques utilisant les émissions secondaires : fluorescence X/diffusion X, luminescence optique et rendement électronique total. Il s'est révélé possible ainsi de rationaliser un certain nombre d'observations expérimentales et de déterminer les conditions opératoires les plus appropriées.

Abstract. — This paper is reviewing a number of artefactual limitations in the current EXAFS analysis. In conventional absorption measurements, the major sources of errors are the transmission of harmonics by the monochromator and inevitable leakages of radiation around or through the sample. The consequences are an alteration of the amplitude of the signal but also some harmonic distortion of the EXAFS oscillations and a systematic perturbation of the measured Debye-Waller terms. An efficient correction of the effects of X-ray leakage is suggested whereas the presence or the elimination of harmonics can be assessed by monitoring the reproducibility of the edge jump when calibrated metallic foils of different nature are inserted behind the sample. The basic analysis developed for absorption measurements has been successively extended to the case of REFLEXAFS and various emission techniques : X-ray fluorescence/scattering, optical luminescence and total electron yield. It became possible to rationalize a number of experimental observations and to determine appropriate operating conditions.

1. **Introduction.** — EXAFS spectroscopy is being used to an increasing extent as a powerful structural tool for the determination of the local atomic arrangement around a given X-ray absorbing centre. Accurate interatomic distances are indeed available from this technique, but it is often difficult to extract from the experimental spectra, reliable values of the coordination number N_c^j or the mean relative displacement σ^j of the jth shell [1]. Besides well known theoretical limitations in the analysis of the pheno-

(†) L.U.R.E. : Laboratoire pour l'Utilisation du Rayonnement Electromagnétique.

menon, e.g. the oversimplified description of the inelastic losses inside the absorbing atom [2] or the arbitrary chosen k-dependence of the photoelectron mean free path, one should often incriminate a number of experimental artefacts [2-5] :

(i) smearing of the EXAFS oscillations due to an unsufficient energy resolution of the monochromator [3],

(ii) contamination of the output beam of the monochromator with higher order reflections but also polychromatic scattered radiations,

(iii) X-ray leakage around the sample holder,

(iv) effects of sample heterogeneity.

In this paper, we wish to review these latter effects and give a detailed quantitative analysis of their consequences on the usual EXAFS absorption spectra. These consequences may become quite dramatic for dense absorbing samples such as amorphous metallic materials. Possible corrections of these effects denaturing the information content of the amplitude of the EXAFS oscillations will then be discussed. Finally, specific aspects of the other modes of detection of the EXAFS structure by reflectivity measurements, X-ray fluorescence or optical luminescence will be shortly considered.

2. **Absorption measurements.** — A bothersome problem in any kind of EXAFS experiment is the transmission by the monochromator of harmonics $N_n(\lambda/n)$ in addition to the primary beam $N_1(\lambda)$. Other unwanted reflections on high order crystallographic plans (e.g. 331/664... in the case of Ge(111) channel cut monocrystals [7]) may also generate spurious beams $N_q(\lambda/q)$ especially at grazing incidence when the output slits of the monochromator are not shut down enough. The output beam of the monochromator is also often contaminated by some scattered polychromatic residual background $N_s(\lambda_s)$, the contribution of which ($\sim$ 1 % ?) is easily detectable with a completely detuned two-crystal monochromator. Obviously, the sample itself is expected to alter the ratio $\rho_i = N_i/N_1$ ($i \neq 1$) as a consequence of the energy dependence of the relevant absorption coefficients (e.g. $\mu_n(E_n) \ll \mu_1(E_1)$).

X-ray leakage around the sample or *via* micropores in it will be further assumed to affect a variable fraction $(1 - y)$ of the total incident beam. For the sake of simplicity in analysing the consequences of some microheterogeneity (e.g. granularity) of a material, we shall postulate a gaussian distribution of the optical path d around the mean value $\bar{d}$ with the variance σ_d^2. Another major concern here is the detector linearity : at high photon fluxes, electron/ion recombination processes may alter the response of the front ionization chamber (I_0) if the nature of the filling gas and/or the applied voltage are not well selected. Thus, within the frame of the present analysis, the currents I_0 and I detected by the two ionization chambers will be written :

$$I_0 = \alpha_1^0 N_1[1 + \beta_q^0 \rho_q + \beta_s^0 \rho_s - \gamma_1^0 N_1] = \\ = \alpha_1^0 N_1[1 + \xi_0] \quad (1a)$$

$$I = \alpha_1^1 y N_1 \exp\{ - \mu_1 \bar{d} + \tfrac{1}{2} \mu_1^2 \sigma_d^2 \}[1 + \xi] \quad (1b)$$

where α_i^j, β_i^j, γ_i^j are unknown coefficients depending only upon the design of the ion chambers and where ξ is now to be splitted as :

$$\xi = \exp\{ \mu_1 \bar{d} - \tfrac{1}{2} \mu_1^2 \sigma_d^2 \} \sum_p \eta_p \quad (2)$$

with :

$$\left.\begin{aligned} \eta_y &= \frac{1 - y}{y} && \text{(leakage of X-rays)} \\ \eta_q &= \beta_q^1 \rho_q \left[\frac{1 - y}{y} + \exp\left\{ - \mu_q \bar{d} + \frac{1}{2} \mu_q^2 \sigma_d^2 \right\} \right] && \text{(harmonics + higher order reflexions)} \\ \eta_s &= \int \beta_s^1 \rho_s \left[\frac{1 - y}{y} + \exp\left\{ - \mu_s \bar{d} + \frac{1}{2} \mu_s^2 \sigma_d^2 \right\} \right] d\lambda_s && \text{(polychromatic background)} \\ \eta_F &= \frac{\varepsilon_F(\Omega/4\pi)\, \mu_1^a}{\mu_1 - \mu_F} [e^{-\mu_F \bar{d}} - e^{-\mu_1 \bar{d}}] \simeq \frac{\varepsilon_F(\Omega/4\pi)\, \mu_1^a}{\mu_1 - \mu_F} e^{-\mu_F \bar{d}} && \text{(sample fluorescence)} \end{aligned}\right\} \quad (3)$$

The latter term which describes the fluorescence of the sample in the direction of propagation should lead to a detectable contribution only for dense, high Z materials, as the fluorescence yield ε_F in a solid angle Ω increases as $\propto Z^4$. In this formulation, μ_F denotes the absorption coefficient at the fluorescence wavelength λ_F, whereas μ_1^a refers to the absorption coefficient of the primary absorption process. Depending upon the geometry of the detector and its proximity : $0.001 < \Omega/4\pi < 0.5$, the sample gives rise to some scattering in the direction of propagation, but its contribution :

$$\eta_{sc} \simeq \sigma(\Omega/4\pi) \bar{d} \exp\{ - \mu_{sc} \bar{d} \} \quad (4)$$

is more rapidly damped out as $\mu_{sc} \gg \mu_F$ and can hardly be detectable.

Defining now the *apparent* absorption coefficient as :

$$\mu_A \bar{d} = -\ln \frac{I}{I_0} = \mu_1 \bar{d} - \frac{1}{2}\mu_1^2 \sigma_d^2 - \ln \frac{1+\xi}{1+\xi_0} - \ln y \frac{\alpha_1^1}{\alpha_1^0} \quad (5)$$

the EXAFS oscillations $\chi(E)$ are then easily introduced by splitting μ_1 into :

$$\mu_1 = \mu_1^b + \mu_1^0(1+\chi) = \mu_1^b + \mu_1^a \quad (6)$$

where μ_1^b and μ_1^0 denote here respectively the pre-edge smooth background absorption and the expected edge jump.

We next wish to expand $\mu_A(\chi)\bar{d}$ as a function of χ in Taylor series :

$$\mu_A(\chi)\bar{d} = \mu_A(0)\bar{d} + \chi\bar{d}\left[\frac{\partial \mu_A}{\partial \chi}\right]_{\chi=0} + \frac{1}{2}\chi^2 \bar{d}\left[\frac{\partial^2 \mu_A}{\partial \chi^2}\right]_{\chi=0} + \cdots \quad (7)$$

For the sake of simplicity, we shall neglect here the weak χ dependence of $\eta_F(\chi)$ and retain the major contribution of the positive exponential in (2). Defining ε_a as $\xi(\chi \equiv 0)$ and ε_b as $\xi(\mu_1^0 \equiv 0)$, a straightforward calculation gives :

$$\mu'_A \bar{d} = \left[\frac{\partial \mu_A}{\partial \chi}\right]_{\chi=0} \bar{d} = \mu_1^0 \bar{d}\left[\frac{1-\mu_1 \sigma_d^2/\bar{d}}{1+\varepsilon_a}\right] = \mu_1^0 \bar{d}\left[\frac{s}{1+\varepsilon_a}\right] \quad (8a)$$

$$\mu''_A \bar{d} = \left[\frac{\partial^2 \mu_A}{\partial \chi^2}\right]_{\chi=0} \bar{d} = -\{\mu_1^0 \bar{d}\}^2 \times \left[\{1-\mu_1 \sigma_d^2/\bar{d}\}^2 \frac{\varepsilon_a}{(1+\varepsilon_a)^2} + \left\{\frac{\sigma_d}{\bar{d}}\right\}^2 \frac{1}{1+\varepsilon_a}\right] \quad (8b)$$

both quantities being, of course, energy dependent. The apparent edge jump is now given at $E = E_0$ by :

$$\mu_A^0 \bar{d} = \mu_1^0 \bar{d}\left[1 - \frac{1}{2}\{\mu_1^0 + 2\mu_1^b\}\frac{\sigma_d^2}{\bar{d}} - \frac{1}{\mu_1^0 \bar{d}} \ln \frac{1+\varepsilon_a}{1+\varepsilon_b}\right] \quad (9)$$

and we may renormalize the amplitude of the EXAFS oscillations simply with respect to this edge jump and thus the first and second order terms to be considered here are :

$$T_1(E)\,\chi(E) = [\mu'_A(E)/\mu_A^0(E_0)]\,\chi$$
$$T_2(E)\,\chi^2(E) = \tfrac{1}{2}[\mu''_A(E)/\mu_A^0(E_0)]\,\chi^2 . \quad (10)$$

It is highly desirable to know the energy dependence of these corrective terms T_1 and T_2. At this stage, it is quite helpful to use the fit coefficients tabulated by McMaster *et al.* [8] for the energy dependence of the scattering and photoelectric cross section according to :

$$\sigma = \sum_{i=0}^{3} A_i (\ln E)^i . \quad (11)$$

These parameters A_i make it possible to expand any $\mu_i(E)$ as :

$$\mu_i \bar{d} = \mu_i(E_0)\bar{d} + P_i(E_0)\frac{E-E_0}{E_0} + \frac{1}{2}Q_i(E_0)\left[\frac{E-E_0}{E_0}\right]^2 + \cdots \quad (12a)$$

and to evaluate numerically P_i and Q_i. In practice, it is more interesting to introduce the photoelectron wave-vector k :

$$\mu_i \bar{d} = \mu_i(k=0)\bar{d} + P_i a^2 k^2 + \tfrac{1}{2} Q_i a^4 k^4 \quad (12b)$$

where $a^{-2} = 2mE_0/\hbar^2$ still keeps here the same meaning as in a recent paper by Lengeler and Eisenberger [3] in which the k-dependence of $\mu_1^0 \bar{d}$ was described by :

$$\mu_1^0 \bar{d} = \mu_1^0(0)\bar{d}\left\{1 - \frac{8}{3}a^2 k^2\right\} \quad \text{for} \quad k < 16\ \text{Å}^{-1} .$$

The final expansion of $T_1(k)$ then becomes :

$$T_1(k) = T_1(k=0) \times \{1 + B_1 a^2 k^2 + C_1 a^4 k^4 + \cdots\} \quad (13)$$

with :

$$B_1 = -P_1\left[\frac{s\varepsilon_a}{1+\varepsilon_a} + \frac{1}{s}\left\{\frac{\sigma_d}{\bar{d}}\right\}^2\right] - \frac{8}{3} + \sum_q \frac{\varepsilon_a s_q}{1+\varepsilon_a}\frac{\eta_q}{\eta}P_q \quad (14a)$$

$$C_1 \simeq -Q_1\left[\frac{s\varepsilon_a}{1+\varepsilon_a} + \frac{1}{s}\left\{\frac{\sigma_d}{\bar{d}}\right\}^2\right] + \frac{1}{2}\left[\left\{\frac{sP_1}{1+\varepsilon_a}\right\}^2 \varepsilon_a\left[\varepsilon_a - 1 - (\varepsilon_a+1)\frac{Q_1}{sP_1^2}\right] + \left\{\frac{\sigma_d}{\bar{d}}\right\}^2 \frac{P_1^2}{1+\varepsilon_a}\left[3\varepsilon_a - (\varepsilon_a+1)\frac{Q_1}{sP_1^2}\right]\right] . \quad (14b)$$

For the sake of simplicity, we neglected, in the latter expression of C_1, the energy dependence of the various η_q contributions. Similar coefficients could be derived for the expansion of $T_2(k)$ but they are of little interest here as we are more interested in a direct numerical evaluation of $T_2(k)$.

It becomes now quite clear that the coordination numbers N^j derived from any current EXAFS analysis have to be corrected by the factor $T_1^0 = T_1(0)$

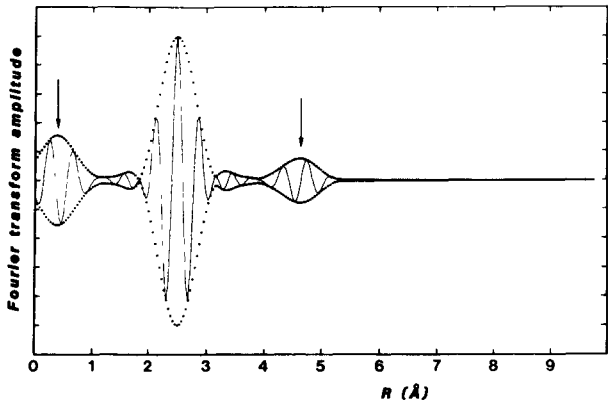

Fig. 1. — Imaginary part (full line) and absolute value (dotted line) of the Fourier transform of the simulated EXAFS spectrum of Co_3B restricted to $R < 3$ Å and backcorrected for the atomic phase-shifts [1b]. The additional signals below 1 Å and at ~ 5 Å are the echoes of the main peak due to the χ^2 contribution ($\bar{d} = 20$ μm ; $\sigma_d = 4$ μm : $\eta_y = 0.06$; $\beta_2 \rho_2 = 0.018$; $\beta_3 \rho_3 = 0.002$; $\varepsilon_F(\Omega/4\pi) = 0.0165$).

whereas the Debye-Waller factor $[\sigma^j]^2$ needs also to be corrected for the systematic error :

$$\Delta[\sigma^j]^2 \simeq -\tfrac{1}{2}\{B_1 + \tfrac{8}{3}\} a^2 .$$

Obviously, the correction $-\frac{8}{3} a^2$ is a direct consequence of the renormalization procedure introduced in equation (10). Beside these primary effects, we expect also, as a consequence of equation (10), the Fourier transformed spectra $\tilde{\chi}(R)$ to be distorted both at very short distances ($R \sim 0$) and large ones ($R > 2 R_1$) by the spectral harmonics associated with $T_2\, \chi^2(k)$. Figure 1 gives a typical illustration of such artefactual contributions for a rather thick, very inhomogeneous crystalline sample of Co_3B ($\bar{d} = 20$ μm ; $\sigma_d \simeq 4$ μm), quite a high level of harmonics ($\beta_2 \rho_2 \simeq 1.8 \times 10^{-2}$; $\beta_3 \rho_3 \simeq 0.2 \times 10^{-2}$), a rather strong proportion of holes ($\eta_y \simeq 0.06$) and some contamination due to the fluorescence of the sample ($\varepsilon_F \simeq 0.33$; $\Omega/4\pi \simeq 0.05$). In order to make the effects more visible, we have restricted our simulation only to the first few shells of the radial distribution ($R < 3$ Å) [1b, 9]. Following a now standard procedure [1b], the exhibited Fourier transformed spectra are corrected for the phase-shifts and amplitude attenuation relative to the first Co*...Co shell. Due to the $T_2\, \chi^2(k)$ term, we observe a kind of « echo » of the intense first peak at about twice the distance of the first shell. This nonlinear term $T_2\, \chi^2(k)$ also induces some perturbation at very short distances ($R \sim 0$).

Figures 2A, 2B, 2C, 2D display respectively the variations with $\mu_1 \bar{d}$ of T_1^0, $T_2^0 = T_2(0)$, $\Delta[\sigma^j]^2$ and the edge jump $\mu_A^0 \bar{d}$. T_2^0 is reaching its maximum value for $\mu_1 \bar{d} \simeq 4.5$ but the ratio T_2^0/T_1^0 keeps growing continuously with $\mu_1 \bar{d}$. Other authors have already emphasized the dramatic effects of holes in a thick or very absorbing sample [6].

For heterogeneous or granular samples, an estimation of σ_d^2 is required. Let n be the number of granules

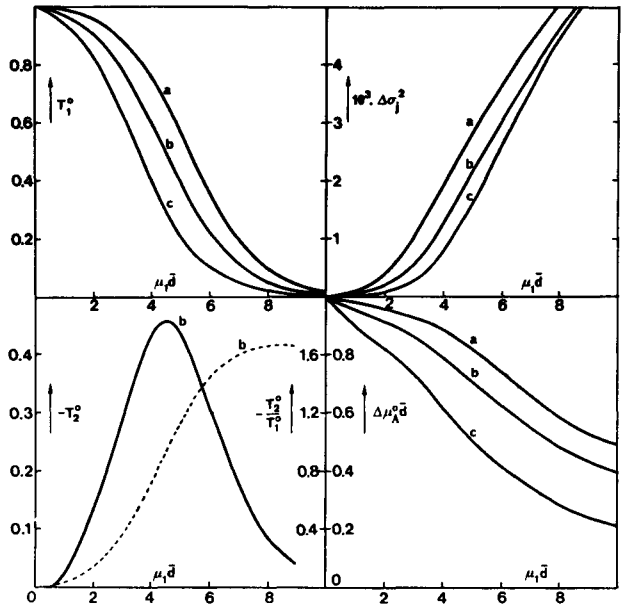

Fig. 2. — Thickness effect on T_1^0 (A), T_2^0 (B), $\Delta[\sigma^j]^2$ (C) and the edge jump $\Delta\mu_A^0 \bar{d}$ (D) for simulated spectra of Co_3B :
a) $\eta_y = 0.0$, $\beta_2 \rho_2 = 0.010$, $\beta_3 \rho_3 = 0.001$, $\varepsilon_F(\Omega/4\pi) = 0.005$.
b) $\eta_y = 0.0$, $\beta_2 \rho_2 = 0.018$, $\beta_3 \rho_3 = 0.002$, $\varepsilon_F(\Omega/4\pi) = 0.015$.
c) $\eta_y = 0.05$, $\beta_2 \rho_2 = 0.010$, $\beta_3 \rho_3 = 0.001$, $\varepsilon_F(\Omega/4\pi) = 0.005$.
The dotted line of figure B is the plot of the quantity T_2^0/T_1^0.

encountered along a particular path :

$$\sigma_d^2 = \sum^n P_n[n \langle e^2 \rangle + n(n-1) \langle e \rangle^2] \quad (15)$$

where P_n denotes the probability of finding n granules of random size e. If P_n is a Poisson distribution, then according to Bowman *et al.* : $\sigma_d^2 = \bar{n} \langle e^2 \rangle$. For granules of uniform thickness $\bar{e}$, this result reduces to : $\sigma_d^2 = \overline{ne}^2$ with $\bar{d} = \overline{ne}$. On the other hand, the σ_d dependence of T_1^0, T_2^0, $\Delta[\sigma^j]^2$ and $\mu_A^0 \bar{d}$ is illustrated by the results quoted in table I for the above considered Co_3B sample. It is worth noticing that for $\sigma_d/\bar{d} < 0.3$, the heterogeneity of the sample gives rise to some attenuation of the effects of the harmonics.

3. **Reduction of the artefacts due to holes and harmonics.** — Obviously, it is highly recommendable to minimize in the experimental setup the various contributions to ξ. Of course, whenever it is possible, the thickness of the sample should be kept thin enough ($\mu_1 \bar{d} < 2$) whereas carefully adjusted slits behind the sample should help in reducing η_s, η_F and η_y even at the expense of some loss of photons. The use of a two independent crystals monochromator opens new possibilities for the focalization of the X-ray beam thus reducing the sample inhomogeneities and for the rejection of the harmonics if the parallelism of the two crystals is slightly detuned [11-13]. In this configuration, a rotation of one of the crystals in its plan might also eliminate some unwanted Bragg reflections. At low photon energy, a mirror with an appropriate cutoff energy could also contribute to clean up the output beam of the monochromator. Again at the expense of some loss of signal, the sensitivity of ion chambers to harmonics can be easily

Table I. — *Illustration of the σ_d dependence of the quantities T_1^0, T_2^0, $\Delta[\sigma^j]^2$ and $\mu_A^0 \bar{d}$.*

$\sigma_d(\mu)$	T_1^0	$-T_2^0$	$\Delta[\sigma^j]^2$	$\mu_A^0 \bar{d}$	$Co_3B : \bar{d} = 20\ \mu m$
0.0	0.37_6	0.43_2	$21._6 \times 10^{-4}$	0.70_8	$\beta_2 \rho_2 = 0.018$
2.0	0.39_5	0.42_0	$20._1 \times 10^{-4}$	0.70_0	$\beta_3 \rho_3 = 0.002$
4.0	0.44_5	0.36_0	$16._1 \times 10^{-4}$	0.67_2	$\eta_y = 0.0$
6.0	0.47_4	0.26_8	$12._4 \times 10^{-4}$	0.60_8	$\varepsilon_F = 0.33$
8.0	0.29_2	0.27_3	$27._7 \times 10^{-4}$	0.48_2	$\Omega/4\pi = 0.05$
10.0	-0.85	0.63_7	$-31._9 \times 10^{-4}$	0.27_3	

reduced using shorter lengths and/or lighter gas filling.

However, in a number of cases (e.g. laboratory EXAFS facilities), all the required precautions cannot be taken and it then becomes desirable to correct the data in order to compensate, at least partially, the effects discussed above. Let us first indicate a procedure which does not require any accurate evaluation of the various η_p of equation (3) but has proved to be quite efficient in reducing the artefacts due to holes or X-ray leakage around or through the sample.

Let $J(E) = I(E)/I_0(E)$ denote the ratio of the measured quantities I and I_0 defined by equations (1*a*), (1*b*), and let $J_B(E_0)$ be the extrapolated value at $E = E_0$ of the pre-edge contribution to $J(E)$. If $J_0(E) \equiv J(E, \chi \equiv 0)$ refers to the smooth background contribution to $J(E)$ beyond $E = E_0$, it is then convenient to introduce the transformed quantity $G(E)$:

$$G(E) = \frac{J_B(E_0) - J(E)}{J_B(E_0) - J_0(E_0)} \qquad (16a)$$

which can be easily developed as :

$$G(E) = \frac{1}{\Delta_0}\left[1 - \exp\{-Z(\chi)\}\left\{1 - \frac{\Delta\xi_0(E)}{1 + \xi_0(E_0)} + \right.\right.$$

$$\left.\left. + \sum^{p} \delta_p \exp\left[\mu_1 \bar{d} - \frac{1}{2}\mu_1^2 \sigma_d^2\right]\right\}\right] \qquad (16b)$$

where the simplifying notations have been used :

$$Z(\chi, E) = \mu_1^0(E)\,\bar{d}(1 + \chi) + \Delta\mu_1^b(E) -$$

$$- \tfrac{1}{2}[\{\mu_1(E)\}^2 - \{\mu_1^b(E_0)\}^2]\,\sigma_d^2 \qquad (17a)$$

$$\Delta\xi_0 = \xi_0(E) - \xi_0(E_0); \quad \Delta\mu_1^b = \mu_1^b(E) - \mu_1^b(E_0);$$

$$\Delta\eta_p = \eta_p(E) - \eta_p(E_0) \qquad (17b)$$

$$\Delta_0 = 1 - \exp\{-Z(E \equiv E_0; \chi \equiv 0)\} \qquad (17c)$$

$$\delta_p = \eta_p(E_0)\left[\frac{\Delta\eta_p}{\eta_p(E_0)} - \frac{\Delta\xi_0}{1 + \xi_0(E_0)}\right]. \qquad (17d)$$

A corrected pseudo absorption coefficient $\mu_B(E, \chi)$ can thus be defined by :

$$\mu_B(E, \chi) = -\ln\{1 - G(E)\,\Delta_0\} \qquad (18)$$

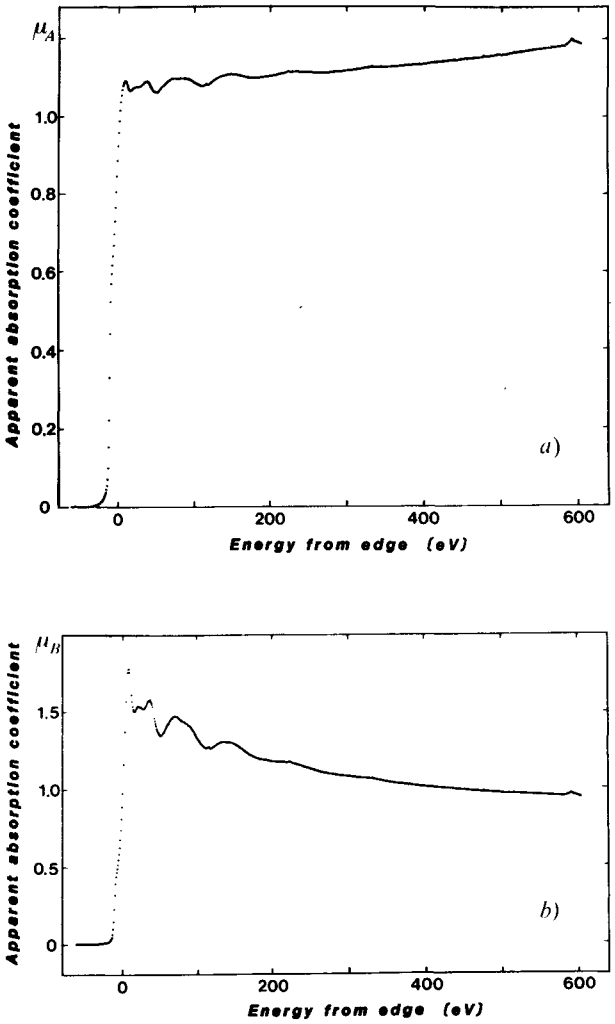

Fig. 3. — Experimental EXAFS spectrum of a broken pellet of Co_3B. X-ray leakage through the sample was rather large. *a*) Conventional analysis. *b*) New procedure.

and its numerical evaluation requires only rough estimations of the parameters $\bar{d}$ and σ_d involved in the calculation of Δ_0, the quantities μ_1^0, μ_1^b being directly available from the McMaster's tables. The standard analysis of the EXAFS oscillations can now be performed on μ_B with the major advantage that this quantity is less sensitive to the afore discussed artefacts as in most cases $\delta_p \ll \eta_p$. The effects of X-ray leakage can be virtually eliminated if $\Delta\xi_0$ is small enough, as obviously $\Delta\eta_y \equiv 0$.

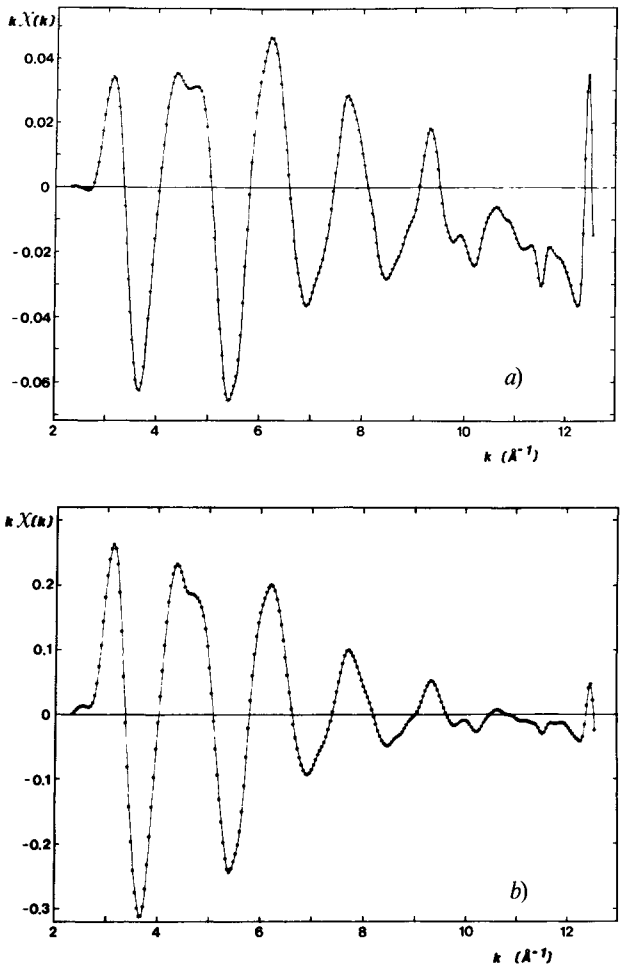

Fig. 4. — EXAFS oscillations of the same broken pellet of Co_3B but after background removal. *a*) Conventional analysis. *b*) New procedure. The apparent reduction of the Bragg « glitch » at ~ 12.6 $Å^{-1}$ should be noticed.

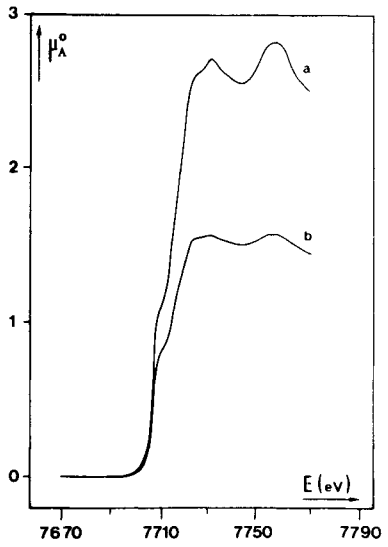

Fig. 5. — Non reproducibility of the near edge spectrum of a cobalt foil (spectrum *a*) when an additional iron foil is inserted (spectrum *b*). The pre-edge contribution has been removed.

In order to illustrate the rather spectacular improvements achievable by this technique, we have reproduced on figures 3*a* and 3*b* the two EXAFS spectra obtained on processing the same data either with the standard analysis or with the new one. The corresponding sample was a broken pellet of Co_3B featuring appreciable X-ray leakage. The EXAFS oscillations after removal of the smooth background are also reproduced on figures 4*a* and 4*b* and it is interesting to notice the *apparent* reduction of the « glitch » observable at around 12.6 $Å^{-1}$.

We next propose a procedure which can help to assess the level of harmonics or of other high order, spurious reflections. We suggest simply to monitor the reproducibility of the amplitude of the edge jump of a test sample (e.g. a calibrated foil of cobalt) when additional calibrated foils of a lower Z element (e.g. Fe, Mn, Cr, Ti) are inserted in front or behind the sample. Although $\mu_1^0 \bar{d}$ remains unchanged, a significant reduction of the edge jump is expected according to equation (9) if the contamination of the beam by high energy photons is important. A typical illustration of such a behaviour is examplified by figures 5*a* and 5*b*. However in interpreting these experiments, one should keep in mind that even if the procedure is basically insensitive to any leakage of radiation around or through the sample itself, the existence of microholes in the added foils can also result in a similar reduction $\Delta\mu_A^0$.

Finally, let us call the attention onto another important limitation of the EXAFS experiments carried out with synchrotron radiation : as the source point is usually very far away from the entrance slits of the monochromator (typically 22 m for DCI), even a small instability of the orbital plan of the electrons in the storage ring can induce a perceptible shift of the beam height. This may be a serious problem for very narrow or locally heterogeneous samples as the beam does not intercept always the same portion of the sample.

4. Surface EXAFS measurements by total reflections of X-rays. — « Total » reflection measurements have proved to be a very useful way of gaining structural informations on the local environment of atoms lying close to the surface. Let us denote the complex refractive index as :

$$n^* = 1 - \delta - i\beta \tag{19}$$

and recall that its imaginary part β is related to the absorption coefficient $\mu_1(\lambda)$ by the standard expression $\beta = \mu_1 \lambda/4\pi$, whereas δ will be assumed here to be nearly proportional to λ^2, as far as the anomalous dispersion contributions can be neglected [14] :

$$\delta \simeq N \frac{e^2}{2\pi m_e c^2} \rho \frac{Z}{M} \lambda^2 \tag{20}$$

where N, e, m_e, c, ρ, Z and M are the standard notations of reference [14].

As long as the X-ray glancing angle Φ will remain lower than the critical value $\Phi_c = \sqrt{2\,\delta}$, the surface will act as a reflecting mirror with a penetration depth of the order of 20 Å [14] and a reflectivity $R < 1$ given at the energy E by :

$$R = \frac{h - a\Phi E\sqrt{2(h-1)}}{h + a\Phi E\sqrt{2(h+1)}} \qquad (21a)$$

where :

$$h = a^2\,\Phi^2\,E^2 + \sqrt{(a^2\,\Phi^2\,E^2 - 1)^2 + b^2\,\mu_1^2\,E^2} \qquad (21b)$$

$$a\Phi_c\,E = 1 \qquad (21c)$$

$$b\mu_1\,E = \frac{\beta}{\delta} \qquad (21d)$$

a and b being obviously two constant parameters depending only on the nature of the sample.

The sensitivity of R with respect to the EXAFS modulation is related to the quantity :

$$S = \frac{1}{R}\frac{dR}{d\chi} = \frac{2(h-2)\,ab^2\,\Phi\mu_1\,\mu_1^0\,E^3}{\sqrt{2(h-1)}\,[h - a^2\,\Phi^2\,E^2]\,[h^2 - 2\,a^2\,\Phi^2\,E^2(h-1)]} \qquad (22)$$

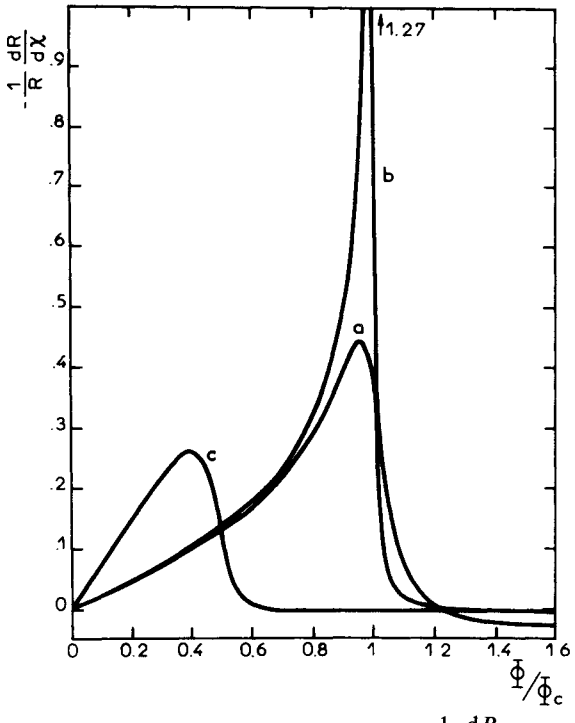

Fig. 6. — Variation of the sensitivity $S = \frac{1}{R}\frac{dR}{d\chi}$ with the glancing angle Φ in the typical case of a copper foil. *a*) The linear absorption coefficient $\mu_1(E)$ has been calculated for an energy lying slightly beyond the edge ($E_0 \simeq 8\,980$ eV). *b*) $\mu_1(E)$ is taken slightly before the edge. *c*) $\mu_2(E)$ has been calculated for $E = 2\,E_0$ (typical sensitivity of the experiment to the second harmonic).

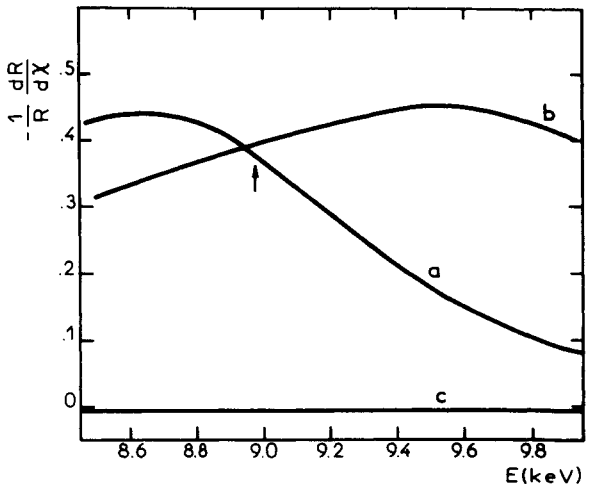

Fig. 7. — Energy dependence of $S(E)$ assuming $\mu_1 \simeq 2\,450\ \text{cm}^{-1}$.

a) $\Phi = \Phi_c$. *b*) $\Phi = 0.95\ \Phi_c$. *c*) $\Phi = \Phi_c$ but the sensitivity refers to the second harmonic at twice the quoted energy. The K-edge of copper is marked by a small arrow.

μ_1^0 keeping here the same meaning as in the previous sections. Our major concern will be to optimize this quantity and to minimize the contribution of the harmonics (λ/n) on varying Φ. In order to illustrate this possibility, we have calculated the values of S as a function of Φ, E and μ_1 for a most typical copper foil sample. From the results displayed on figures 6 and 7, it becomes obvious that the choice of Φ is quite critical : if $\Phi > 1.1\ \Phi_c$, R becomes fully insensitive to the EXAFS modulation χ, the same situation occurring also for small values of Φ. The best sensitivity and simultaneously the best harmonic rejection are in fact achieved for $\Phi/\Phi_c \simeq 0.95$: the level of $\lambda/2$ harmonics is kept below 2 % whereas (Fig. 7)

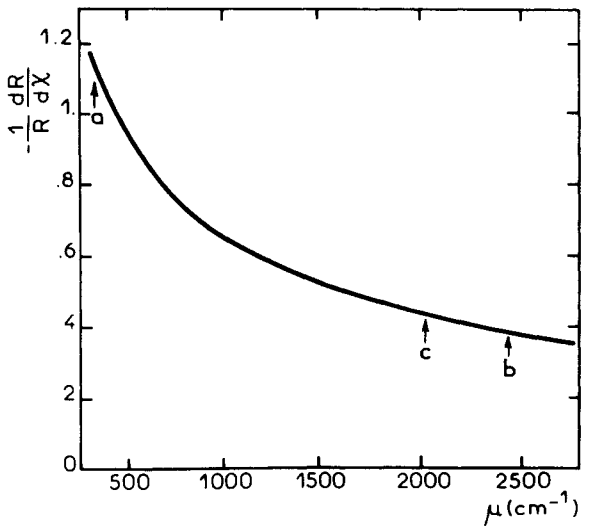

Fig. 8. — Variations of $S(\Phi = \Phi_c, E = E_0)$ with μ_1. The arrows again refer to selected values of μ_1 : *a*) below the edge, *b*) above the edge, *c*) at the edge.

S remains high over the whole energy range, as opposed to the rather rapid decay of $S(E)$ predicted for $\Phi = \Phi_c$. It should be noticed that for the sake of clarity, the smooth energy dependence of $\mu_1(E)$ and $\mu_1^0(E)$ were neglected, but the corresponding effects are expected to be very small (Fig. 8).

Our conclusions are apparently well supported by a detailed investigation of the nice set of experimental results reported recently by Martens and Rabe [15]. Moreover, one may expect some slight enhancement of the sensitivity of the experiment in the close vicinity of an absorption edge as a consequence of the anomalous dispersion terms contributing to δ.

5. **Emission EXAFS spectroscopy.** — 5.1 X-RAY FLUORESCENCE/SCATTERING. — For the sake of simplicity, we shall restrict here our analysis to the X-ray induced emission associated with a planar, rather thick pellet of an absorbing sample. In a geometrical arrangement where the incident and emission radiations make respectively the angles Φ and Ψ with the planar surface of the pellet, the counting rate in the particular direction Ψ is given by :

$$F(\Psi) = \sum_{j=1}^{q} \frac{N_j \sigma_F^j \varepsilon_F (\Omega/4\pi)}{\mu_j(E_j) + \mu_F(E_F) \sin\Phi/\sin\Psi} \times \times \left[1 - \exp\left\{ - \frac{\mu_j \bar{d}}{\sin\Phi} - \frac{\mu_F \bar{d}}{\sin\Psi} \right\}\right] \quad (23)$$

where the summation is over the fundamental and the harmonics of the incident beam. Here σ_F denotes the absorption coefficient associated with the primary absorption process resulting in the present emission with the quantum yield ε_F. This expression does not hold only for the X-ray fluorescence ($\sigma_F^1 = \mu_1^0(1 + \chi)$), but it is also representative of the X-ray scattering emission of the sample provided that one is replacing σ_F by σ_{sc} and $\mu_F(E_F)$ by $\mu_1(E_{sc})$. For thick samples, the exponential factors can often be neglected. We may further observe that the relative contribution of the harmonics scales as $\sim \rho_q \mu_q^0/\mu_1^0$ for dilute systems and can hardly be larger than 0.02 : the low level, smooth background emission excited by the harmonics is not usually a major source of error.

It is now of some interest to check what may happen when the X-ray fluorescence signal is burried into an intense coherent ($E_{sc} \simeq E$) scattering emission. The corresponding edge jump is then given by :

$$F^0(\varepsilon_F, \sigma_{sc}^{coh}) = \frac{\mu_1^0 N_1}{\mu_1^0 + \mu_1^b + \alpha_F \mu_F} \times \times \left[\varepsilon_F - \frac{\sigma_{sc}^{coh}}{(1 + \alpha_F)\mu_1^b} \left\{ 1 + \frac{\alpha_F \mu_F}{\mu_1^0 + \mu_1^b} \right\}\right] \quad (24)$$

where $\alpha_F = \sin\Phi/\sin\Psi$. The next step requires the evaluation of the partial derivatives :

$$\frac{\partial F}{\partial \chi} = \frac{\mu_1^0 N_1}{\mu_1^0 + \mu_1^b + \alpha_F \mu_F} \left[\varepsilon_F \left\{ 1 - \frac{\mu_1^0}{\mu_1^0 + \mu_1^b + \alpha_F \mu_F} \right\} - \frac{\sigma_{sc}^{coh}}{(1+\alpha_F)(\mu_1^0 + \mu_1^b)} \left\{ 1 + \frac{\alpha_F \mu_F}{\mu_1^0 + \mu_1^b} \right\} \right] \quad (25a)$$

$$\frac{1}{2} \frac{\partial^2 F}{\partial \chi^2} = \frac{\mu_1^{0^2} N_1}{[\mu_1^0 + \mu_1^b + \alpha_F \mu_F]^2} \left[\varepsilon_F \left\{ 1 - \frac{\mu_1^0}{\mu_1^0 + \mu_1^b + \alpha_F \mu_F} \right\} - \frac{\sigma_{sc}^{coh}}{(1+\alpha_F)(\mu_1^0 + \mu_1^b)} \left\{ 1 + \frac{\alpha_F \mu_F}{\mu_1^0 + \mu_1^b} \right\}^2 \right]. \quad (25b)$$

Thus, X-ray scattering does not give rise only to the dramatic degradation of the noise statistics of the detector as discussed by many authors [17, 19] : it still induces some attenuation of both the edge jump F^0 and the EXAFS oscillations. This reduction of the signal also contributes to a further degradation of the signal/noise ratio. Fortunately, the leading factor $\sigma_{sc}/\varepsilon_F \mu_1^b$ can hardly be larger than 0.3 and therefore this effect has never a dramatic intensity. It is however certainly advisable to try to filter out the contribution of X-ray scattering [17-20].

As far as coordination numbers are concerned, the contribution of X-ray scattering is of little effect as a partial compensation is introduced on considering the normalized quantity : $\frac{1}{F^0} \frac{\partial F}{\partial \chi}$

$$\frac{1}{F^0} \frac{\partial F}{\partial \chi} \simeq 1 - \frac{\mu_1^0}{\mu_1^0 + \mu_1^b + \alpha_F \mu_F} + + \frac{\sigma_{sc}^{coh} \alpha_F \mu_F \mu_1^0}{\varepsilon_F (1 + \alpha_F) \mu_1^b (\mu_1^0 + \mu_1^b)^2} + \cdots \quad (26)$$

It is however apparent from equation (26) that, even in the absence of scattering, large corrections would be required if the fluorescence technique was to be used for studying concentrated samples for which $\mu_1^0 \geqslant \mu_1^b + \alpha_F \mu_F$. It can still be shown from equation (25*b*) that the second order term $\propto \chi^2$ is also reaching its maximum value for $\mu_1^0 \simeq \mu_1^b + \alpha_F \mu_F$.

5.2 X-RAY EXCITED OPTICAL LUMINESCENCE (XEOL). — It has been recognized for a long time that a number of elements [21, 22] (e.g. rare-earth cations), if placed in appropriate environments, had a strong emission of UV-visible radiations when excited by X-ray photons. It was shown recently by Bianconi *et al.* [23] that this emission provided an alternative way of detecting EXAFS oscillations in these systems. One of the advantages of the method is lying in the ability of designing an appropriate optics collecting the photons in a very large solid angle and free of X-ray scattered emission [24]. We feel essential however to emphasize the variable and fairly complex nature of the multielectron processes following the primary X-ray absorption. In practice, the relationship (23)

can still be used but $\varepsilon_F\ \sigma_F$ is now to be splitted into a χ dependent and a χ independent part :

$$\varepsilon_F\ \sigma_F = \varepsilon_L^1\ \mu_1^0(1 + \chi) + \varepsilon_L^2\ \mu_1^b \qquad (27)$$

where the pseudo-quantum yields ε_L^1 and ε_L^2 are not usually identical as they should be governed by different selection rules which apply to the relevant electron transitions. Having regards to the complexity of the multielectron rearrangement involved, there is little hope to achieve any definitive estimations of ε_L^1 or ε_L^2, but the formal description (26) makes it already possible to predict positive (e.g. ZnO) [25] or inversed (e.g. CaF_2) [23] manifestations of the near edge and extended fine structure (EXAFS) oscillations without postulating any dubious, detailed mechanism for the electron relaxation following the X-ray absorption [23].

Indeed, if we assume that the sample is thick enough to neglect the exponential term in equation (23), but that it is also nearly transparent to optical radiations, i.e. $\mu_F \sim 0$ (e.g. CaF_2), then the edge jump is given by :

$$F_L^0(\gamma) = \frac{\mu_1^0\ N_1}{\mu_1^0 + \mu_1^b + \alpha_F\ \mu_F} \times$$

$$\times \left[\varepsilon_L^1 - \varepsilon_L^2 \frac{\mu_1^b}{\mu_1^b + \alpha_F\ \mu_F}\right] \simeq \frac{\mu_1^0\ N_1}{\mu_1^0 + \mu_1^b}(\varepsilon_L^1 - \varepsilon_L^2) \qquad (28)$$

and is positive if ε_L^1 is dominant (e.g. ZnO) but negative in the alternative case (CaF_2).

As in the previous sections, we are interested in the Taylor series expansion of $F_L(\chi)$ and thus in the quantities :

$$\frac{\partial F_L}{\partial \chi} = F_L^0(\varepsilon_L^1, \varepsilon_L^2) \frac{\mu_1^b + \alpha_F\ \mu_F}{\mu_1^0 + \mu_1^b + \alpha_F\ \mu_F} \simeq F_L^0 \frac{\mu_1^b}{\mu_1^0 + \mu_1^b} \qquad (29a)$$

$$\frac{1}{2}\frac{\partial^2 F}{\partial \chi^2} = F_L^0(\varepsilon_L^1, \varepsilon_L^2) \frac{\mu_1^0(\mu_1^b + \alpha_F\ \mu_F)}{[\mu_1^0 + \mu_1^b + \alpha_F\ \mu_F]^2} \simeq$$

$$\simeq F_L^0 \frac{\mu_1^0\ \mu_1^b}{[\mu_1^0 + \mu_1^b]^2}. \qquad (29b)$$

It is noteworthy that the normalized quantities $\frac{1}{F_L^0}\frac{\partial F}{\partial \chi}$ or $\frac{1}{F_L^0}\frac{\partial^2 F}{\partial \chi^2}$ are not anymore dependent upon ε_L^1, ε_L^2 or upon the positive/negative nature of the spectra. However if, as suggested by Bianconi *et al.*, this technique is to be used for studying monocrystals of concentrated materials, the same corrections as for X-ray fluorescence are indeed required as strong distortions of the spectra can result from equation (29*b*).

An important question is whether or not this technique might afford some further selectivity between non equivalent sites of a given absorbing element. From equations (23) and (27), one is led to give certainly a negative answer if ε_L^2 is the dominant factor : the various sites contribute to the oscillating nature of the X-ray absorption coefficient $\mu_1(E)$ which appears at the denominator of equation (23). In the alternative case, the answer is not so clear cut and may still be positive. The very high sensitivity of the optical fluorescence technique makes it anyway worth being developed.

5.3 SURFACE ELECTRON EMISSION. — The total yield of electrons at the surface of a X-ray excited sample includes both rather energetic electrons (such as direct photoelectron, inelastically scattered electrons, photoelectrons resulting from a reabsorption near the surface of X-ray fluorescence photons,...) and low energy electrons such as Auger or secondary electrons associated with non radiative relaxation processes of the core hole. As the mean free path of the latter low energy electrons amounts to only a few angströms, the structural informations achieved by an energy resolved detection of the Auger electron yield [26, 27] will be characteristic of a few atomic layers, but at the expense of a severe limitation of sensitivity. Much simpler and promising with respect to sensitivity appears the detection of the total electron yield which however is reflecting structural informations relevant to a penetration depth as large as 1 000-2 000 Å due to the reabsorption process of X-ray fluorescence. Equation (23) still does apply to the total (or partial) electron yield, but with a few adaptations :

- At small glancing angles, N_j is better replaced by $N_j(1 - R_j)$ where $R_j(E_j, \chi)$ denotes again here the reflectivity of the surface to the incoming X-ray beam.
- $\varepsilon_y^1\ \mu_1^0(1 + \chi) + \varepsilon_y^2\ \mu_1^b$ should replace, as for optical luminescence, the quantity $\varepsilon_F\ \sigma_F$.
- $\mu_y(E')$, i.e. the inverse of the escape depth of the electrons ($\sim$ 5 Å at 100 eV; $\sim$ 50 Å at 10 keV; $\sim$ 1 000 Å for reabsorbed X-ray fluorescence) containing the structural information is to be substituted to $\mu_F(E_F)$.

For small glancing angles ($\sin \Phi \ll 1$) the penetration of X-ray photons decreases and the yield of photoelectron increases. Furthermore one may observe that for small glancing angles, the exponential term of equation (23) vanishes as well as the leading coefficient $\alpha = \sin \Phi / \sin \Psi$ of the rather embarrassing quantity $\mu_y(E')$ and finally :

$$Y = \sum_j N_j(1 - R_j) \frac{\varepsilon_y^1\ \mu_j^a(\chi) + \varepsilon_y^2\ \mu_j^b}{\mu_j^a(\chi) + \mu_j^b}. \qquad (30)$$

For $\Phi > \Phi_c$, $R_j \simeq 0$ and the problem is shown thus to be formally identical to the case of optical luminescence discussed above : one may easily predict a rapid attenuation of both the edge jump and the EXAFS oscillations together with a strong

harmonic distortion (χ^2) of the spectra if $\mu_1^0 \geqslant \mu_1^b$, i.e. for concentrated samples such as metallic surfaces. This was already noticed by Rabe and Haensel [6]. The method is more suitable for studying diluted species lying near the surface.

For $\Phi \lesssim \Phi_c$, the total electron yield is providing an alternative measure of the surface reflectivity $R(\chi)$, especially for concentrated samples or metallic surfaces. The considerations already developed above are still valid here.

6. **Conclusion.** — We have reviewed in this paper a number of artefactual limitations in the current EXAFS analysis. In the most conventional absorption mode of detection of the EXAFS oscillations, the pollution of the monochromatic beam by harmonics or any kind of photons of different energy is a major source of difficulty together with inevitable X-ray leakage around or through the sample. Dramatic effects can be predicted and observed, especially for very thick samples. Very recently, a somewhat similar but incomplete discussion of these effects was first given by Stern and Kim [28] but our slightly different analytical approach brings into evidence new aspects of the problem such as the χ^2 harmonic distortion of the spectra and the variation of the Debye-Waller factors. Also an original correction is suggested in order to get rid of the artefacts due to the leakage of radiation around the sample or through microholes. On the other hand, the harmonic contamination of the output beam of the monochromator can be controlled or even assessed from the non reproducibility of the edge jump on inserting behind the sample additional foils of other absorbers.

The same general analysis, i.e. a Taylor series expansion of any kind of measured quantity $Q(\chi)$, has been furthermore applied to a discussion of reflectivity EXAFS measurements and of various types of emission EXAFS techniques : X-ray fluorescence/scattering, optical luminescence and total electron yield. It has been possible to rationalize a number of experimental observations and to determine the most appropriate conditions of operation for each experiment.

Acknowledgments. — This work was financially supported by the C.N.R.S. (L.U.R.E., ERA 22, GR IV, LA 159). It is also worth mentioning here many fruitful discussions with the EXAFS group at L.U.R.E. Finally, we are indebted to the staff of the Laboratoire de l'Accélérateur Linéaire d'Orsay for running DCI during dedicated beam time.

References

[1] a) Goulon-Ginet, C., Thèse d'Etat, Université de Nancy I (1979).
b) Dubois, J. M., Thèse d'Etat, Institut National Polytechnique de Lorraine (1981).
[2] Stern, E. A., Heald, S. M. and Bunker, B., *Phys. Rev. Lett.* **42** (1979) 1372.
[3] Lengeler, B. and Eisenberger, P., *Phys. Rev. B* **21** (1980) 4507.
[4] Eisenberger, P. and Lengeler, B., *Phys. Rev. B* **22** (1980) 3551.
[5] Werner, A., Ph. D. Thesis, University of Kiel (1979).
[6] Rabe, P. and Haensel, R., Festkörper Probleme XX (*Adv. in Solid State Physics*) (1980) 43, J. Treusch ed., Braunschweig.
[7] Petiau, J., *Notice à l'intention des utilisateurs des monochromateurs channel-cut* Si(220) *et* Ge(111) *de L.U.R.E.* (1977).
[8] McMaster, W. H., Kerr del Grande, N., Mallett, J. H. and Hubbell, J. H. (N.B.S.), « Compilation of X-ray Cross Sections » Sec. II, Rev. 1, N.T.I.S. (U.S. Dept. of Commerce) 5285 Port Royal Road, Springfield, VA 22151.
[9] Rundqvist, S., *Acta Chem. Scand.* **12** (1958) 658.
[10] Beaumont, J. H. and Hart, M., *J. Phys. E* 7 (1974) 823.
[11] Hart, M. and Rodrigues, A. R. D., *J. Appl. Crystallogr.* **11** (1978) 248.
[12] Mills, D. and Pollock, V., *Rev. Sci. Instrum.* **51** (1980) 1664.
[13] Bowman, J. D., Kankeleit, E., Kaufmann, E. N. and Persson, B., *Nucl. Instrum. Methods* **50** (1967) 13.
[14] Parrat, L. G., *Phys. Rev.* **95** (1954) 359.
[15] Martens, G. and Rabe, P., *Phys. Status Solidi A* **58** (1980) 415.
[16] Jaklevic, J. J., Kirby, J. A., Klein, M. P., Robertson, A. S., Brown, G. S. and Eisenberger, P., *Solid State Commun.* **23** (1977) 679.
[17] Stern, E. A. and Heald, S. M., *Rev. Sci. Instrum.* **50** (1979) 1579.
[18] Marcus, M., Powers, L. S., Storm, A. R., Kincaid, B. M. and Chance, B., *Rev. Sci. Instrum.* **51** (1980) 1023.
[19] Hastings, J. B., « EXAFS of Dilute Systems. Fluorescence Detection », Chap. 11 in *EXAFS Spectroscopy. Techniques and Applications*, B. K. Teo and D. C. Joy eds. (Plenum Press) 1981.
[20] Hastings, J. B., Eisenberger, P., Lengeler, B. and Perlman, M. L., *Phys. Rev. Lett.* **43** (1979) 1807.
[21] Makowski, J., Low, W. and Yatsiv, S., *Phys. Lett.* **2** (1962) 186.
[22] D'Silva, A. P. and Fassel, V. A., *Anal. Chem.* **45** (1973) 542.
[23] Bianconi, A., Jackson, D. and Monahan, K., *Phys. Rev. B* **17** (1978) 2021.
[24] Tola, P., Lemonnier, M. and Goulon, J., to be published.
[25] Greegor, R. B., Lytle, F. W. and Sandstrom, D. R., SSRL, Users Group Meeting (1977).
[26] Citrin, P. H., Eisenberger, P. and Hewitt, R. C., *Phys. Rev. Lett.* **41** (1978) 309.
[27] Stohr, J., Johansson, L., Lindau, J. and Pianetta, P., *Phys. Rev. B* **20** (1979) 664.
[28] Stern, E. A. and Kim, K., *Phys. Rev. B* **23** (1981) 3781.